The Infrared Spectrum of F⁻·H₂O

Brian F. Yates,*,† Henry F. Schaefer III,† Timothy J. Lee,⊥,§ and Julia E. Rice⊥,§,‡

Contribution from the Center for Computational Quantum Chemistry,‡ School of Chemical Sciences, University of Georgia, Athens, Georgia 30602, and Department of Chemistry, University of California, Berkeley, California 94720. Received January 28, 1988

Abstract: Ab initio molecular electronic structure methods have been used in conjunction with high-quality basis sets to determine the geometry and vibrational frequencies of the F⁻·H₂O system at the self-consistent-field (SCF) and configuration interaction with single and double excitation (CISD) levels of theory. At the CISD level, the largest basis set used was triple-ζ with two sets of polarization functions and a set of diffuse functions (TZ2P + diff). Anharmonic corrections were determined at the SCF level with a complete quartic force field. In addition, a one-dimensional CISD potential energy surface corresponding to the vibrational mode with the largest predicted infrared intensity (ν_2, the asymmetric F–H–O stretch) has been evaluated. Significant deviations from the harmonic approximation are found. At the CISD/TZ2P + diff level of theory, the ω_2 harmonic vibrational frequency is 2670 cm⁻¹ for F⁻·H₂O and 1955 cm⁻¹ for F⁻·D₂O. With the inclusion of anharmonic effects, the ν_2 fundamental frequencies are predicted to be 1853 cm⁻¹ (F⁻·H₂O) and 1481 cm⁻¹ (F⁻·D₂O). The calculations confirm that the F⁻·H₂O system is strongly hydrogen bonded and is therefore a likely candidate to be observed via high-resolution infrared spectroscopy.

I. Introduction

The realm of gas-phase infrared spectroscopy has undergone rapid advancement in recent years with the development of high-resolution techniques for measuring the vibrational frequencies of gas-phase ions.[1,2] Although a large number of cations have now been studied, it is only recently that the techniques have been extended to include molecular anions.[3-11] Of those molecules that might be classified as anionic clusters, the F⁻·H₂O complex is found experimentally to have one of the stronger binding energies (23.3 kcal mol⁻¹)[12] and so should be a likely candidate to be observed by the high-resolution IR techniques. Because of the high-resolution nature of the experiment, it would be desirable if theory could provide some estimate of the location of the fundamental vibrational frequencies of the complex.

Previous theoretical studies of the F⁻·H₂O system have included complete self-consistent-field (SCF) geometry optimizations with several small basis sets (without diffuse functions).[13-16] Partial geometry optimizations have also been performed with a variety of theoretical methods,[17-23] including the use of fairly large basis sets[20] and configuration interaction (CI).[21] Numerous estimates have been made of the binding energy of the complex with respect to F⁻ + H₂O.[13-28] With the largest basis sets[20] and with inclusion of electron correlation,[21] the ab initio methods yielded good agreement between theory and experiment. Although there have been several estimates of the nature of the potential surface for F⁻·H₂O,[15,16,20,21,24,27,29-33] there has been no thorough ab initio study of all the vibrational frequencies of the complex. Kistenmacher et al.[29] obtained some approximate frequencies for one conformation of the complex (which, as they noted, is not the minimum energy isomer); however, their sole aim was to determine vibrational corrections to thermodynamic quantities. Harmonic and anharmonic estimates for the two lowest energy vibrational frequencies (corresponding to intermolecular motions) have also been computed by Janoschek.[32]

The goal of the present work is to determine accurate anharmonic vibrational frequenies for the F⁻·H₂O complex with ab initio techniques. The theoretical challenge is 3-fold: first, it is generally acknowledged[34-36] that a proper theoretical description of the molecular properties of anions requires more effort (larger basis sets, more extensive treatments of electron correlation) than that required for similar cationic or neutral species; second, the floppy nature of cluster molecules and the resulting "flat" potential energy surfaces require that extra care be taken in evaluating an adequate

representation of the potential surface; and third, the F–H–O stretching frequency is expected to be highly anharmonic.

(1) Oka, T. *Phys. Rev. Lett.* **1980**, *45*, 531.

(2) Gudeman, C. S.; Saykally, R. J. *Annu. Rev. Phys. Chem.* **1984**, *35*, 387.

(3) Kawaguchi, K.; Hirota, E. *J. Chem. Phys.* **1986**, *84*, 2953.

(4) Rosenbaum, N. H.; Owrutsky; J. C.; Tack, L. M.; Saykally, R. J. *J. Chem. Phys.* **1986**, *84*, 5308.

(5) Rehfuss, B. D.; Crofton, M. W.; Oka, T. *J. Chem. Phys.* **1986**, *85*, 1785.

(6) Tack, L. M.; Rosenbaum, N. H.; Owrutsky, J. C.; Saykally, R. J. *J. Chem. Phys.* **1986**, *85*, 4222.

(7) Gruebele, M.; Polak, M.; Saykally, R. J. *J. Chem. Phys.* **1987**, *86*, 1698.

(8) Polak, M.; Gruebele, M.; Saykally, R. J. *J. Am. Chem. Soc.* **1987**, *109*, 2884.

(9) Gruebele, M.; Polak, M.; Saykally, R. J. *J. Chem. Phys.* **1987**, *86*, 6631.

(10) Gruebele, M.; Polak, M.; Saykally, R. J. *J. Chem. Phys.* **1987**, *87*, 1448.

(11) Polak, M.; Gruebele, M.; Saykally, R. J. *J. Chem. Phys.* **1987**, *87*, 3352.

(12) Arshadi, M.; Yamdagni, R.; Kerbarle, P. *J. Phys. Chem.* **1970**, *74*, 1475.

(13) Alagona, G.; Scrocco, E.; Tomasi, J. *Theor. Chim. Acta* **1978**, *47*, 133.

(14) Emsley, J.; Parker, R. J.; Overill, R. E. *J. Chem. Soc., Faraday Trans. 2* **1983**, *79*, 1347.

(15) Donnella, J.; Murdoch, J. R. *J. Am. Chem. Soc.* **1984**, *106*, 4724.

(16) Sapse, A. M.; Jain, D. C. *Int. J. Quant. Chem.* **1985**, *27*, 281.

(17) Diercksen, G. H. F.; Kraemer, W. P. *Chem. Phys. Lett.* **1970**, *5*, 570.

(18) Lischka, H.; Plesser, T.; Schuster, P. *Chem. Phys. Lett.* **1970**, *6*, 263.

(19) Russegger, P.; Lischka, H.; Schuster, P. *Theor. Chim. Acta* **1972**, *24*, 191.

(20) Kistenmacher, H.; Popkie, H.; Clementi, E. *J. Chem. Phys.* **1973**, *58*, 5627.

(21) Diercksen, G. H. F.; Kraemer, W. P.; Roos, B. O. *Theor. Chim. Acta* **1975**, *36*, 249.

(22) DeKock, R. L.; Caswell, D. S. *J. Phys. Chem.* **1981**, *85*, 2639.

(23) Gao, J.; Garner, D. S.; Jorgensen, W. L. *J. Am. Chem. Soc.* **1986**, *108*, 4784.

(24) Breitschwerdt, K. G.; Kistenmacher, H. *Chem. Phys. Lett.* **1972**, *14*, 288.

(25) Kollman, P.; McKelvey, J.; Johansson, A.; Rothenberg, S. *J. Am. Chem. Soc.* **1975**, *97*, 955.

(26) Sauer, J.; Hobza, P. *Theor. Chim. Acta* **1984**, *65*, 291.

(27) Gowda, B. T.; Benson, S. W. *J. Comput. Chem.* **1983**, *4*, 283.

(28) Cieplak, P. Lybrand, T. P.; Kollman, P. A. *J. Chem. Phys.* **1987**, *86*, 6393.

(29) Kistenmacher, H.; Popkie, H.; Clementi, E. *J. Chem. Phys.* **1973**, *59*, 5842.

(30) Kolos, W. *Theor. Chim. Acta* **1979**, *51*, 219.

† University of Georgia.
⊥ University of California.
§ Present address: University Chemical Laboratory, Lensfield Road, Cambridge CB2 1EW, United Kingdom.
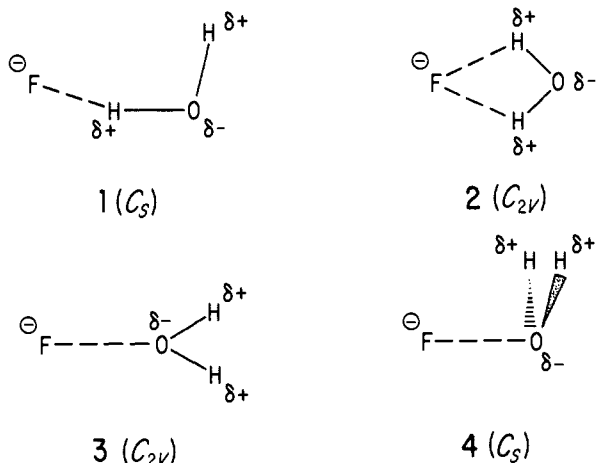‡ CCQC contribution No. 7.

Figure 1. Possible structures for the complex of F^- with H_2O.

Figure 2. Internal coordinates employed in the study of complexes **1** and **2**.

II. Theoretical Methods

Previous studies of vibrational frequencies of anions[34,37] have shown the importance of using flexible basis sets incorporating polarization and diffuse functions. Four basis sets of this type were used in our study and may be labeled TZP+diff, TZ2P+diff, TZ4P+diff, and TZ4P+diff+d. Full details are presented in the Appendix. The largest basis set resulted in 132 basis functions for $F^-\cdot H_2O$.

A selection of possible geometries for the $F^-\cdot H_2O$ complex is displayed in Figure 1. Structures **3** and **4** have been shown[20] to be unbound and were not considered in this work. Geometries for **1** and **2** were optimized (to 10^{-6} Å or radians for the internal coordinates) at the single determinant Hartree–Fock (HF) level of theory by using the basis sets mentioned above (only two of the basis sets, TZ2P+diff and TZ4P+diff+d, were employed for structure **2**). Harmonic vibrational frequencies (and quadratic force constants) were obtained at this level through the analytic evolution of second derivatives.[41] Infrared intensities were calculated from analytic dipole moment derivatives.[42,43]

Geometry optimizations for **1** were also carried out by using the complete active space (CAS) SCF method[44,45] as implemented in the CADPAC program.[46] The valence electronic configuration of **1** is

$$\dots (3a')^2(4a')^2(5a')^2(6a')^2(1a'')^2(7a')^2(2a'')^2(8a')^2$$

The active space was chosen to be the six valence a' molecular orbitals occupied in the reference configuration ($3a'$–$8a'$) together with the first four virtual a' orbitals ($9a'$–$12a'$). (The two valence π orbitals were thus constrained to be doubly occupied in all configurations.) The CASSCF method includes all possible excitations within this active space and leads to 44 100 configurations.

Further geometry optimizations incorporating electron correlation were carried out with use of the configuration interaction (CI) formalism and the TZ2P+diff basis set. All valence-shell single and double excitations were included in the CI expansions (CISD) with the two lowest-lying molecular orbitals (oxygen and fluorine 1s-like orbitals) restricted to be doubly occupied and the corresponding two virtual orbitals left unoccupied in all configurations. This resulted in 103 821 configurations for structure **1** and 53 445 configurations for **2**. The CISD ge-
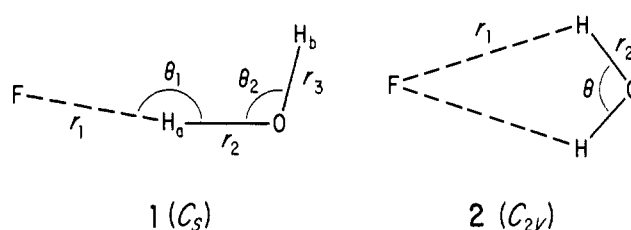
ometries were determined by using a shape driven graphical unitary group approach CI method[47] with analytical gradients.[48,49] Improved relative energies including contributions from unlinked quadruple excitations to the CISD energies were estimated by using the formula of Davidson[50,51] and results including this estimate are denoted by CIDVD. Harmonic vibrational frequencies were determined for **1** at the CISD/TZ2P+diff level via finite differences of analytic first derivatives.

No attempt was made in this work to evaluate the effects of basis set superposition errors (BSSE). Although such effects may be important in determining accurate interaction energies, they are likely to play only a minor role in the determination of geometries and vibrational frequencies compared to the errors in these properties that would arise from, say, the truncation of the basis set or an incomplete incorporation of electronic correlation.

Cubic force constants for **1** were obtained through analytic evaluation of third derivatives[52] at the HF/TZP+diff level of theory with use of the HF/TZP+diff optimized geometry. A complete set of quartic force constants was obtained for **1** via finite differences of the analytic third derivatives. The finite difference displacements were performed in symmetry internal coordinates (defined below), and the resulting quartic force field curvilinearly transformed[53] into Cartesian coordinates.

The effects of anharmonicity on the vibrational frequencies of **1** were investigated with two methods. First, anharmonic constants x_{rs} were evaluated by using the full quartic force field and standard second-order perturbation theory.[52,54,55] Fundamental frequencies were then obtained from the relation

$$\nu_r = \omega_r + 2x_{rr} + \frac{1}{2}\sum_{s\ne r} x_{rs}$$

Although it is somewhat unclear as to how well this method might be expected to perform for weakly bound complexes (see, for example, the study on HCN–HF by Amos et al.[56]), the results from the perturbation treatment are included here for comparison with other methods.

Our second method for treating the anharmonicity in $F^-\cdot H_2O$ was to determine a one-dimensional potential energy curve corresponding to Q_r (the r-th normal coordinate), fit this curve to a Taylor series, and then determine vibrational energy levels from numerical solution of the one-dimensional vibrational Schrödinger equation.[57–59] Since in one dimension the vibrational energy levels for an anharmonic system may be expressed as

$$G_r(v) = \omega_r(v + \tfrac{1}{2}) + x_{rr}(v + \tfrac{1}{2})^2 + \dots$$

(31) Sadlej, J. *Adv. Mol. Relax. Interact. Proc.* **1979**, *15*, 163.

(32) Janoschek, R. *J. Mol. Struct.* **1982**, *84*, 237.

(33) Larson, J. W.; McMahon, T. B. *J. Am. Chem. Soc.* **1983**, *105*, 2944.

(34) Lee, T. J.; Schaefer, H. F. *J. Chem. Phys.* **1985**, *83*, 1784.

(35) Simons, J.; Jordan, K. D. *Chem. Rev.* **1987**, *87*, 535.

(36) Nobes, R. H.; Poppinger, D.; Li, W.-K.; Radom, L. In *Comprehensive Carbanion Chemistry, Part C*; Buncel, E., Durst, T., Eds.; Elsevier: Amsterdam, 1987; Chapter 1.

(37) Janssen, C. L.; Allen, W. D.; Schaefer, H. F.; Bowman, J. M. *Chem. Phys. Lett.* **1986**, *131*, 352.

(38) Van Duijneveldt, F. B. *IBM Res. Dept. RJ* **1971**, *945*, A2, A53, A63.

(39) Table I of ref 34.

(40) Reference 38; p A65.

(41) Saxe, P.; Yamaguchi, Y.; Schaefer, H. F. *J. Chem. Phys.* **1982**, *77*, 5647.

(42) Amos, R. D. *Chem. Phys. Lett.* **1984**, *108*, 185.

(43) Yamaguchi, Y.; Frisch, M.; Gaw, J.; Schaefer, H. F.; Binkley, J. S. *J. Chem. Phys.* **1986**, *84*, 2262.

(44) Roos, B. O.; Taylor, P. R.; Siegbahn, P. E. M. *Chem. Phys.* **1980**, *48*, 157.

(45) Werner, H. J.; Knowles, P. J. *J. Chem. Phys.* **1985**, *82*, 5053.

(46) Amos, R. D.; Rice, J. E. CADPAC: Cambridge Analytic Derivatives Package; developed at Cambridge University (England) under the direction of Dr. Nicholas C. Handy.

(47) Saxe, P.; Fox, D. J.; Schaefer, H. F.; Handy, N. C. *J. Chem. Phys.* **1982**, *77*, 5584.

(48) Osamura, Y.; Yamaguchi, Y.; Schaefer, H. F. *J. Chem. Phys.* **1982**, *77*, 383.

(49) Rice, J. E.; Amos, R. D.; Handy, N. C.; Lee, T. J.; Schaefer, H. F. *J. Chem. Phys.* **1986**, *85*, 963.

(50) Davidson, E. R. In *The World of Quantum Chemistry*; Daudel, R., Pullman, B., Eds.; Reidel: Dordrecht, Holland, 1974; p 17.

(51) Langhoff, S. R.; Davidson, E. R. *Int. J. Quantum Chem.* **1974**, *8*, 61.

(52) Gaw, J. F.; Yamaguchi, Y.; Schaefer, H. F.; Handy, N. C. *J. Chem. Phys.* **1986**, *85*, 5132.

(53) The curvilinear transformations between internal and Cartesian coordinates were performed directly and analytically with the INTDER program written by Dr. W. D. Allen. Details of the procedure are available upon request.

(54) Mills, I. M. In *Molecular Spectroscopy: Modern Research*; Rao, K. N., Mathews, C. W., Eds.; Academic: New York, 1972; pp 115–140.

(55) Clabo, D. A.; Allen, W. D.; Remington, R. B.; Yamaguchi, Y.; Schaefer, H. F., submitted for publication.

(56) Amos, R. D.; Gaw, J. F.; Handy, N. C.; Simandiras, E. D.; Somasundram, K. *Theor. Chim. Acta* **1987**, *71*, 41.

(57) Cooley, J. W. *Math. Comp.* **1961**, *15*, 363.

(58) Cashion, J. K. *J. Chem. Phys.* **1963**, *39*, 1872.

(59) Zare, R. N. University of California Radiation Laboratory Report UCRL-10925; 1963.

Table I. Optimized Geometries[a] and Total Energies (hartree) for F⁻·H₂O

basis set	level of theory	geometrical parameters, structure 1 (C_s)					
		r_1	r_2	r_3	θ_1	θ_2	total energy
TZP+diff	HF	1.482	1.006	0.944	173.4	103.2	−175.541 541
[6s4p1d/4s1p]							
TZ2P+diff	HF	1.500	0.999	0.939	174.5	103.7	−175.560 445
[8s5p2d/4s2p]	CASSCF	1.448	1.033	0.959	176.0	102.6	−175.656 025
	CISD	1.453	1.022	0.949	175.5	102.8	−176.018 787
TZ4P+diff	HF	1.495	0.999	0.938	174.6	103.6	−175.561 021
[8s5p4d/4s3p]							
TZ4P+diff+d	HF	1.490	1.000	0.938	174.7	103.6	−175.562 081
[8s5p4d/4s3p1d]							
6-31G[b]	HF	1.41	1.04	0.95	171.2	107.6	
6-31G(d,p)[b]	HF	1.38	1.04	0.94	172.9	101.3	
[7s4p1d/4s3p1d/2s1p][c]	HF	1.52	1.000	0.946	175.5	102.7	

basis set	level of theory	geometrical parameters, structure 2 (C_{2v})			
		r_1	r_2	θ	total energy
TZ2P+diff	HF	2.102	0.949	94.3	−175.551 237
	CISD	2.046	0.961	92.2	−176.008 554
TZ4P+diff+d	HF	2.100	0.948	94.2	−175.552 711
6-31G[b]	HF	1.96	0.96	94.3	
6-31G(d,p)[b]	HF	1.91	0.96	88.4	
[7s4p1d/4s3p1d/2s1p][c]	HF	2.146	0.955	95.1	

[a] Bond lengths in Å, angles in deg. [b] From ref 16. [c] [F/O/H], from ref 20.

Table II. Harmonic Vibrational Frequencies (cm⁻¹) and Infrared Intensities in Parentheses (km mol⁻¹) for F⁻·H₂O

Structure 1 (C_s)

basis set	level of theory	ω_1 a′	ω_2 a′	ω_3 a′	ω_4 a′	ω_5 a′	ω_6 a″
TZP+diff	HF	4173 (9)	2936 (1960)	1844 (140)	569 (74)	330 (108)	1160 (165)
TZ2P+diff	HF	4200 (11)	3001 (1817)	1858 (113)	565 (62)	327 (102)	1133 (110)
	CISD	4044 (6)	2670 (2141)	1789 (103)	562 (53)	346 (124)	1125 (80)
TZ4P+diff	HF	4195 (11)	2976 (1829)	1855 (110)	567 (62)	329 (102)	1134 (106)
TZ4P+diff+d	HF	4200 (11)	2961 (1855)	1853 (108)	572 (62)	330 (104)	1143 (106)

Structure 2 (C_{2v})

basis set	level of theory	ω_1 a₁	ω_2 a₁	ω_3 a₁	ω_4 b₁	ω_5 b₁	ω_6 b₂
TZ2P+diff	HF	4083	1775	244	4068	479i	849

Table III. Computed and Experimental Geometries,[a] Harmonic Vibrational Frequencies (cm⁻¹), and Infrared Intensities in Parentheses (km mol⁻¹) for H₂O

basis set	level of theory	r_{O-H}	θ_{HOH}	ω_1 a₁	ω_2 a₁	ω_3 b₁
TZ2P+diff	HF	0.941[b]	106.5[b]	4133[b] (15)	1754[b] (95)	4237[b] (92)
	CISD	0.954	105.1	3927 (6)	1687 (74)	4032 (62)
experiment		0.958[c]	104.5[c]	3832[d] (2)[e]	1648[d] (54)[e]	3943[d] (45)[e]

[a] Bond length in Å, angle in deg. [b] From ref 34. [c] From ref 60. [d] Fron ref 61. [e] From ref 62.

then the separation of the lowest two vibrational energy levels (as determined from the one-dimensional Schrödinger equation) is equivalent to

$$G_r(1) - G_r(0) =$$

$$\omega_r + 2x_{rr} + \text{higher order diagonal anharmonicity terms}$$

This result may be combined with the off-diagonal anharmonicity term ($^1/_2\Sigma_{s\neq r}x_{rs}$) obtained from perturbation theory to yield an estimate for the fundamental frequency, ν_r. Clearly, the advantage of using this method is that it includes the higher order (>2) diagonal anharmonicity terms neglected by second-order perturbation theory.

The simple internal coordinates used in the study of structures **1** and **2** are defined in Figure 2. The symmetry internal coordinates used for **1** are defined as

$$S_1 = \frac{1}{\sqrt{2}}(r_1 + r_2),\; S_2 = \frac{1}{\sqrt{2}}(r_1 - r_2),\; S_3 = r_3,\; S_4 = \theta_1,\; S_5 = \theta_2,\; S_6 = \tau$$

where τ is the torsion angle between the planes defined by the atoms (FH$_a$O) and (H$_a$OH$_b$).

Optimized geometries and total energies for **1** and **2** are presented in Table I and harmonic vibrational frequencies and intensities in Table II. For comparative purposes, the computed and experimental[60–62] geometry

and harmonic vibrational frequencies for H₂O are displayed in Table III. The full quartic force field for **1** in symmetry internal coordinates is contained in Table IV, anharmonic constants are presented in Table V, and fundamental frequencies are given in Table VI.

III. Geometries and Relative Energies

The results in Table I indicate that at the HF level most of the geometrical parameters for **1** change only slightly as the flexibility of the basis set is increased. However, comparison with the previously reported results of Sapse et al.[16] shows that there is a significant lengthening of about 0.1 Å in the F–H distance (r_1) in **1** on going from the smaller 6-31G(d,p) basis set to those used in the present study. Even with the flexible basis sets used here, the F–H distance is found to be somewhat sensitive to the inclusion of multiple sets of polarization functions (Table I); the inclusion of d-type functions on H shortens the F–H distance by 0.005 Å. The CASSCF geometry for **1** exhibits slightly longer O–H bonds

(60) Hoy, A. R.; Bunker, P. R. *J. Mol. Spectrosc.* **1979**, *74*, 1.
(61) Hoy, A. R.; Mills, I. M.; Strey, G. *Mol. Phys.* **1972**, *24*, 1265.
(62) Ziles, B. A.; Person, W. B. *J. Chem. Phys.* **1983**, *79*, 65.

6330 *J. Am. Chem. Soc., Vol. 110, No. 19, 1988*

Yates et al.

Table IV. Quartic Force Field[a] in Symmetry Internal Coordinates[b] for F⁻·H₂O (1)

F_{11}	4.38	F_{41}	0.0200	F_{53}	0.231
F_{21}	-2.44	F_{42}	0.0584	F_{54}	-0.0874
F_{22}	1.95	F_{43}	-0.0428	F_{55}	0.548
F_{31}	-0.0368	F_{44}	0.216	F_{66}	0.00155
F_{32}	0.0320	F_{51}	0.114		
F_{33}	9.14	F_{52}	-0.0532		
F_{111}	-21.3	F_{432}	-0.00268	F_{543}	0.0162
F_{211}	13.4	F_{433}	-0.0935	F_{544}	0.0581
F_{221}	-15.5	F_{441}	-0.355	F_{551}	-0.219
F_{222}	17.7	F_{442}	-0.284	F_{552}	0.560
F_{311}	0.0682	F_{443}	0.00814	F_{553}	-0.212
F_{321}	-0.0774	F_{444}	-0.0539	F_{554}	0.0389
F_{322}	0.00942	F_{511}	-0.0663	F_{555}	-0.537
F_{331}	0.0365	F_{521}	0.0332	F_{661}	-0.00221
F_{332}	0.194	F_{522}	-0.239	F_{662}	0.00523
F_{333}	-65.8	F_{531}	-0.278	F_{663}	-0.00424
F_{411}	-0.168	F_{532}	0.383	F_{664}	-0.0364
F_{421}	-0.111	F_{533}	-0.124	F_{665}	-0.0101
F_{422}	0.0205	F_{541}	0.0696		
F_{431}	0.100	F_{542}	0.00922		
F_{1111}	88.8	F_{4432}	-0.0194	F_{5531}	0.151
F_{2111}	-56.7	F_{4433}	0.00275	F_{5532}	-0.496
F_{2211}	68.8	F_{4441}	0.331	F_{5533}	0.0629
F_{2221}	-69.2	F_{4442}	0.181	F_{5541}	-0.0271
F_{2222}	68.0	F_{4443}	-0.0851	F_{5542}	0.0845
F_{3111}	-0.498	F_{4444}	0.445	F_{5543}	0.00977
F_{3211}	0.396	F_{5111}	0.102	F_{5544}	0.0632
F_{3221}	-0.228	F_{5211}	0.228	F_{5551}	0.498
F_{3222}	0.416	F_{5221}	-0.0891	F_{5552}	-0.485
F_{3311}	-0.0590	F_{5222}	0.248	F_{5553}	0.752
F_{3321}	-0.161	F_{5311}	-0.0128	F_{5554}	0.163
F_{3322}	-0.296	F_{5321}	-0.408	F_{5555}	-0.669
F_{3331}	-0.712	F_{5322}	0.370	F_{6611}	-0.00743
F_{3332}	0.911	F_{5331}	0.341	F_{6621}	-0.00728
F_{3333}	396	F_{5332}	-0.428	F_{6622}	0.000862
F_{4111}	0.962	F_{5333}	-1.12	F_{6631}	0.0112
F_{4211}	0.192	F_{5411}	-0.0241	F_{6632}	0.0000590
F_{4221}	-0.0149	F_{5421}	-0.0424	F_{6633}	-0.0109
F_{4222}	-0.303	F_{5422}	0.112	F_{6641}	0.0268
F_{4311}	-0.322	F_{5431}	-0.105	F_{6642}	-0.0518
F_{4321}	0.0419	F_{5432}	-0.0349	F_{6643}	0.0359
F_{4322}	0.0326	F_{5433}	0.113	F_{6644}	0.0960
F_{4331}	0.0452	F_{5441}	0.0403	F_{6651}	0.00857
F_{4332}	-0.0215	F_{5442}	0.0373	F_{6652}	0.000742
F_{4333}	-0.0141	F_{5443}	-0.0187	F_{6653}	0.00146
F_{4411}	1.35	F_{5444}	0.00370	F_{6654}	0.0922
F_{4421}	0.503	F_{5511}	0.0425	F_{6655}	0.00510
F_{4422}	-0.104	F_{5521}	-0.175	F_{6666}	-0.00549
F_{4431}	-0.0628	F_{5522}	-0.549		

[a] Quadratic force constants from CISD/TZ2P+diff//CISD/TZ2P+diff calculations, cubic and quartic values from HF/TZP+diff//HF/TZP+diff calculations. Non-zero force constants only are listed. [b] Using the symmetry coordinates defined in the text. F_{ij} are in aJ Å⁻², aJ Å⁻¹ rad⁻¹, or aJ rad⁻², F_{ijk} are in aJ Å⁻³, aJ Å⁻² rad⁻¹, aJ Å⁻¹ rad⁻², or aJ rad⁻³, and F_{ijkl} are in aJ Å⁻⁴, aJ Å⁻³ rad⁻¹, aJ Å⁻² rad⁻², aJ Å⁻¹ rad⁻³, or aJ rad⁻⁴ (1 aJ = 1 mdyn Å).

Table V. Anharmonic Constants x_{rs} (cm⁻¹) for F⁻·H₂O, Structure 1[a]

			s			
r	1	2	3	4	5	6
1	-80.14					
2	-17.56	-410.4				
3	-11.50	-27.53	-10.71			
4	-4.397	124.9	-60.50	-9.024		
5	0.234	40.98	-4.116	-10.59	-4.848	
6	0.377	251.4	18.28	-13.05	-19.86	-49.96

[a] Calculated with HF/TZP+diff second, third, and fourth derivatives (see text).

and a wider H–O–H angle than at the HF level. The inclusion of π-electron correlation in the CASSCF wave function would not be expected to change this result greatly. The effect on 1 of including electron correlation at the CISD level is to lengthen both

Table VI. Anharmonic Frequencies (cm⁻¹) for F⁻·H₂O (1), from Perturbation Treatment

harmonic freq (ω)[a]	anharmonicity correction	anharmonic freq (ν)
4044	-177	3867
2670	-635	2035
1789	-64	1725
562	0	562
346	-6	340
1125	19	1144

[a] CISD/TZ2P+diff result from Table II. [b] Calculated from the anharmonic constants in Table V (see text).

of the O–H distances and decrease the F–H distance, although these changes are not as great as in the CASSCF structure. Geometries at both the correlated levels show a marked decrease in r_1. In these calculations the CASSCF and CISD wave functions are dominated by the HF reference configuration ($c_0 = 0.983$, $c_1 = -0.050$ for CASSCF and $c_0 = 0.954$, $c_1 = -0.020$ for CISD).

The results for structure 2 show similar trends as the theoretical model is improved. The smaller basis sets used by Sapse et al.[16] appear to underestimate the F–H distance by nearly 0.2 Å at the HF level, while the inclusion of electron correlation lengthens the O–H distances and shortens the F–H distances (again, the HF reference configuration is dominant in the CISD calculations: $c_0 = 0.954$ and $c_1 = -0.026$).

The geometries of 1 and 2 at the HF/TZ2P+diff level of theory may be compared with the structure of free H₂O calculated at the same level (Table III). The effects of complexation are a distortion of the hydrogen-bonded H (both of them in the case of 2) toward the fluorine anion and a concomitant closing of the H–O–H angle. (The CISD geometries exhibit similar trends.) These effects, together with the contrasting geometries of 1 and 2, are consistent with an analysis of the bonding in F⁻·H₂O previously presented by other workers.[20,23,63]

Although the main thrust of this work is to examine the infrared spectrum of F⁻·H₂O, we note that at the HF/TZ2P+diff level, with thermal and zero-point vibrational energy corrections,[64,65] the binding energy of 1 with respect to F⁻ and H₂O is calculated to be 23.2 kcal mol⁻¹.[66] compared to the experimental ΔH_{298} value of 23.3 kcal mol⁻¹.[12] With the TZ2P+diff basis set, 1 is calculated to be more stable than 2 by 5.8, 6.4 and 6.5 kcal mol⁻¹ at the HF, CISD, and CIDVD levels, respectively.

IV. Infrared Spectrum

The harmonic vibrational frequencies presented in Table II demonstrate some dependency on the inclusion of multiple sets of polarization functions, paralleling the trend in geometrical parameters seen in Table I. The largest fluctuations are seen for ω_2. Inclusion of electron correlation leads to large decreases in ω_1 and ω_2; however, these changes are not atypical (there are similar decreases, although not as large, in the stretching frequencies of H₂O on going from the HF to the CISD level, Table III). A very large infrared intensity is seen for the proton transfer coordiante ω_2 and, although anharmonicity effects may vary this somewhat, this band is still likely to be the first and most easily observed in the infrared spectrum because of the charge redistribution that would occur in this mode.

The vibrational frequencies and corresponding infrared intensities for free H₂O are shown in Table III. The effects of complexation (a large red shift and dramatic increase in intensity of an O–H stretching band) are consistent with the formation in 1 of a strong F–H hydrogen bond.

The vibrational analysis for 2 reveals an imaginary frequency of 479i cm⁻¹. This frequency corresponds to an in-plane rocking

(63) Larson, J. W.; McMahon, T. B. *J. Am. Chem. Soc.* **1984**, *106*, 517.

(64) McQuarrie, D. A. *Statistical Mechanics*; Harper and Row: New York, 1976.

(65) Hehre, W. J.; Radom, L.; Schleyer, P. v. R.; Pople, J. A. *Ab Initio Molecular Orbital Theory*; Wiley: New York, 1986.

(66) At the HF/TZ2P+diff level, $E(\text{H}_2\text{O}) = -76.064632$ and $E(\text{F}^-) = -99.458366$ hartrees.

Table VII. Harmonic Vibrational Frequencies (cm⁻¹) and Infrared Intensities in Parentheses (km mol⁻¹) for F⁻·D₂O (Structure 1)

basis set	level of theory	ω_1 a′	ω_2 a′	ω_3 a′	ω_4 a′	ω_5 a′	ω_6 a″
TZ2P+diff	HF	3055 (*18*)	2193 (*945*)	1352 (*51*)	407 (*24*)	317 (*109*)	815 (*70*)
	CISD	2941 (*5*)	1955 (*1075*)	1302 (*35*)	406 (*17*)	335 (*127*)	809 (*44*)
TZ4P+diff+*d*	HF	3055 (*11*)	2165 (*966*)	1349 (*48*)	412 (*28*)	321 (*111*)	822 (*67*)

of the H₂O group and confirms that **2** represents a transition structure for the interconversion of equivalent structures of **1**.

Combining the anharmonic constants in Table V with the CISD harmonic frequencies (Table II) leads to the predictions for the fundamental frequencies presented in Table VI. The largest anharmonic correction (−635 cm⁻¹) is that calculated for ω_2, yielding a predicted value for ν_2 of 2035 cm⁻¹. While the effect of anharmonicity on the second vibrational mode is undoubtedly large, the size of the correction predicted here suggests that anharmonic terms neglected in the second-order perturbation treatment may be important. Since ω_2 is also the frequency with the largest predicted infrared intensity, it was decided to undertake further studies on the anharmonicity of this mode.

An analysis of the potential energy distributions for the CISD harmonic vibrational frequencies of **1** in terms of the symmetry internal coordinates defined in the Methods section reveals that ω_2 is almost exclusively dominated (99.2%) by the S_2 component. That is, the second normal mode may be fairly accurately described as the asymmetric coupling of the F–Hₐ and Hₐ–O stretches (Figure 2). Thus, one way of investigating the shape of the potential surface for F⁻·H₂O along the ν_2 mode is to calculate the energy of the complex as a function of S_2 while fixing the remaining internal (symmetry) coordinates at their equilibrium values. Such a one-dimensional potential energy curve may be used as described in the Methods section to obtain a more accurate estimate of the anharmonicity correction to ω_2.

The CISD/TZ2P+diff one-dimensional curve is shown in Figure 3. To simplify the calculation of the curve the F–Hₐ–O angle was straightened to 180° (raising the energy by 0.09 kcal mol⁻¹), the F–O distance was fixed at the sum of the F–Hₐ and the Hₐ–O equilibrium distances (2.475 Å at the CISD level), and Hₐ was then displaced about its equilibrium position. The results clearly demonstrate the anharmonicity present in the Q_2 mode. Although no barrier for the proton shift is found, a plateau is seen at r(R–H) = 1.08 Å corresponding to the FH–OH⁻ complex. A sixth-order Taylor series provided an excellent least-squares fit to the CISD curve (negligible improvement with seventh- or eighth-order) and numerical solution of the one-dimensional Schrödinger equation led to the vibrational energy levels: E_0 = 1171.71, E_1 = 2839.05, E_2 = 4139.58, E_3 = 5854.19, and E_4 = 7827.17 cm⁻¹. The separation of the lowest two energy levels is 1667 cm⁻¹. The off-diagonal anharmonicity term ($^1/_2\sum_{s\neq r}x_{rs}$) calculated from perturbation theory is 186 cm⁻¹, whence ν_2 = 1667 + 186 = 1853 cm⁻¹. This is significantly lower than the 2035-cm⁻¹ value obtained from the perturbation treatment.

The results from the solution of the one-dimensional Schrödinger equation lead to another interesting observation. Since E_1 lies at 2839 cm⁻¹, or 0.013 hartree, on the CISD one-dimensional curve (Figure 3), evaluation of the classical turning points suggests that r(F–H) can vary from as little as 0.95 Å to as much as 1.55 Å in the v_2 = 1 vibrationally excited state; i.e., the second normal mode, ν_2, corresponds to a large amplitude vibration.

It is instructive to compare the CISD curve in Figure 3 with the potential energy as obtained from the force field parameters. Using the CISD/TZ2P+diff F_{22} and HF/TZP+diff F_{222} and F_{2222} diagonal force constants from Table IV (in symmetry internal coordinates), we obtain the force field curve shown in Figure 3. Clearly, the force field parameters do not adequately describe the anharmonicity effects away from the equilibrium position. The F_{22}, F_{222}, and F_{2222} force constants are 1.95 aJ Å⁻², 17.7 aJ Å⁻³, and 68.0 aJ Å⁻¹, respectively, while the corresponding coefficients from a least-squares fit of a sixth-order Taylor series to the CISD curve are 1.93 aJ Å⁻², 16.0 aJ Å⁻³, and 69.2 aJ Å⁻⁴. The similarity of these two sets of coefficients suggests that the deficiency in the force field curve could be due to neglect of higher order force
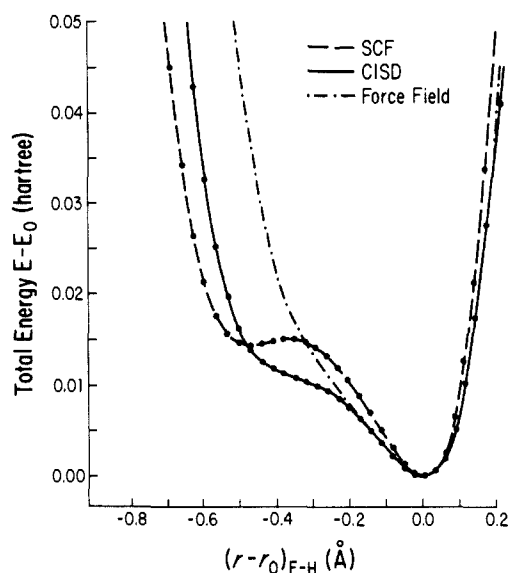

Figure 3. One-dimensional potential energy curves for the second symmetry internal coordinate of F⁻·H₂O (**1**) calculated at the CISD/TZ2P+diff (—) and SCF/TZ2P+diff (- - -) levels of theory, and calculated with the diagonal S_2 force constants (- · ·-); see text for details. E_0 and r_0 are the energies and F–H bond lengths, respectively, of the reference geometries; E_0 = −176.018 637 and −175.560 216 hartree and r_0 = 1.453 and 1.500 Å at the CISD and SCF levels, respectively.

constants. (The higher order coefficients from the sixth-order Taylor series are F_{22222} = 217 aJ Å⁻⁵ and F_{222222} = 728 aJ Å⁻⁶.)

We note in passing that an SCF/TZ2P+diff one-dimensional curve, obtained in an analogous manner to the CISD curve described above, also displays considerable anharmonicity in the S_2 coordinate (Figure 3). This curve is rather different from the much smoother potentials computed at the SCF/4-31G level of theory by other workers.[15,33] There is even a shallow second minimum corresponding to the FH–OH⁻ structure at r(F–H) = 1.020 Å (although this minimum may disappear when the other internal coordinates are relaxed).

The harmonic vibrational frequencies for F⁻·D₂O are shown for several levels of theory in Table VII. At all levels, the most intense mode is ω_2, and at the CISD/TZ2P+diff level this mode has a harmonic vibrational frequency of 1955 cm⁻¹. Using the methods outlined earlier, we calculate an anharmonic correction of −326 cm⁻¹ for this mode (with the off-diagonal term being 90 cm⁻¹). Thus, we obtain values for the ν_2 fundamental frequency of 1629 cm⁻¹ from the perturbation approach and 1481 cm⁻¹ from the solution of a one-dimensional Schrödinger equation with $^1/_2\sum_{s\neq r}x_{rs}$ correction.

V. Concluding Remarks

The theoretical prediction of the anharmonic frequency for the asymmetric F–H–O stretch in F⁻·H₂O is a difficult problem. We have optimized the geometry of the complex and evaluated harmonic vibrational frequencies with flexible basis sets and with the inclusion of electron correlation. At our best level of theory, the F–H–O stretch is predicted to have a harmonic vibrational frequency of 2670 cm⁻¹ and to have a large IR intensity. Even at this level of theory, however, the predicted value for the harmonic frequency may still be too high. The anharmonic correction for this mode is computed to be large and negative and this is likely to be qualitatively correct. Overall, the ab initio prediction that the corresponding anharmonic frequency lies at about 1853 cm⁻¹ could still be an overestimate, and this result may possibly change

with more sophisticated theoretical treatments.

Appendix

In this study the smallest basis set used consists of (a) a triple-ζ (TZ) contraction of Van Duijneveldt's[38] (10s6p) primitive set for O and F and the (6s) primitive set for H according to the scheme (10s6p/6s) $\rightarrow$ [5s3p/3s]; (b) the addition of a set of polarization functions for each atom ($\alpha_d(O) = 0.85$, $\alpha_d(F) = 1.0$, $\alpha_p(H) = 0.75$); and (c) the addition of diffuse s- and p-type functions on O and F $\alpha_s(O) = 0.0840898$, $\alpha_p(O) = 0.0584002$, $\alpha_s(F) = 0.106753$, and $\alpha_p(F) = 0.0709406$; these exponents were obtained in an even tempered sense by using the ratios of the last two exponents of the (10s6p) primitive set and a diffuse s-type function on H ($\alpha_s(H) = 0.030155$[39]). This basis set, labeled TZP+diff,

may be technically designated [6s4p1d/4s1p] and its use results in 62 contracted Gaussian functions (CGFs) for F$^-$·H_2O.

The second basis set is labeled TZ2P+diff. We have previously described the formulation of this set for O and H.[34] The basis set for F is obtained in an exactly analogous manner and consists of a [7s4p] contraction of the (12s7p) primitive set of Van Duijneveldt[40] with the addition of two sets of polarization functions ($\alpha_d = 1.5$ and 0.35) and one set of diffuse s- and p-type functions ($\alpha_s = 0.0978$, $\alpha_p = 0.0649$). The TZ2P+diff basis set may be technically designed [8s5p2d/4s2p] and its use results in 90 CGFs for F$^-$·H_2O.

Basis set three is labeled TZ4P+diff. It consists of the TZ2P+diff set but with four sets of polarization functions on O and F and three sets on H ($\alpha_d = 2.25, 0.75, 0.25,$ and 0.083 for O and F, and $\alpha_p = 1.4, 0.25,$ and 0.083 for H). This basis set may be designated [8s5p4d/4s3p] and results in 120 CGFs for F$^-$·H_2O.

The last basis set used is labeled TZ4P+diff+d and consists of the TZ4P+diff basis set augmented by a set of d-type functions on H ($\alpha_d = 1.0$). Use of this basis set ([8s5p4d/4s3p1d]) results in 132 CGFs.

A Theoretical Study of the Reaction of Ketene Radical Cation with Ethylene: Nucleophilic Addition or Concerted [2 + 1] Cycloaddition?[†]

Nikolaus Heinrich,[†] **Wolfram Koch,**[§] **J. C. Morrow,**[⊥] **and Helmut Schwarz***

Contribution from the Institute of Organic Chemistry, Technical University Berlin, D-1000 Berlin 12, Federal Republic of Germany. Received February 1, 1988

Abstract: A thorough molecular orbital study of the potential energy surface of ionized cyclobutanone reveals that, in line with ESR data, this species does not appear to be a minimum on the MP2/6-31G**//6-31G* + ZPVE potential energy surface. While ring-opening by cleavage of the C(1)/C(2) bond (α-cleavage) has no barrier, the alternative reaction, i.e., cleavage of the C(2)/C(3) bond (β-cleavage), is predicted to be associated with a significant barrier. This is indicated by the fact that the β-cleavage product **4** is higher in energy than the sum of the heats of formation of the fission products C_2H_4 and $C_2H_2O^{•+}$. The reverse reaction, i.e., the formal [2 + 1] cycloaddition of ionized ketene with ethylene, has been analyzed in detail. It has been found that this process should *not* be classified as a cycloaddition reaction but rather as a nucleophilic addition of C_2H_4 to the terminal carbon atom of the ketene radical cation. This type of reaction is governed by a 3-electron/2-orbital interaction as is the case with the recently described[15] nucleophilic addition of NH_3 to ionized ketene. The MO results present for the first time a coherent description of all experimental findings, including ESR studies at 77 K and ion/molecule reactions of $C_2H_4O^{•+}$ with C_2X_4 (X = H, D) in the gas phase.

The reactivity and stereoselectivity patterns in cycloaddition reactions of neutral organic molecules have been impressively accounted for by the Woodward-Hoffmann rules[1] and the Frontier Molecular Orbital (FMO) approach introduced by Fukui.[2] On the basis of simple symmetry considerations and energy differences of interacting molecular orbitals, these models provide a qualitative classification of reactions as being high-("forbidden") and low-energy processes ("allowed"). Much less is known, however, about these features in cycloadditions involving radical cations. As the occupation of the orbitals of reacting species is changed upon ionization, a change of the reaction mechanism is likely to result.[3] The last few years have witnessed a growing interest of both experimentalists and theoreticians on "hole" catalyzed cycloadditions. Bauld and co-workers[4] demonstrated that radical cation

Scheme I
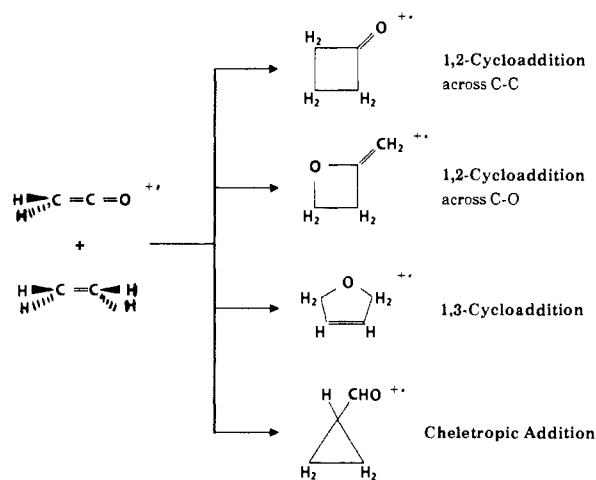
catalyzed Diels-Alder reactions occur with considerably enhanced reaction rates and selectivities, compared to the respective neutral

---